Defect physics of the $CuInSe_2$ chalcopyrite semiconductor

S. B. Zhang, Su-Huai Wei, and Alex Zunger
National Renewable Energy Laboratory, Golden, Colorado 80401

H. Katayama-Yoshida
The Institute of Scientific and Industrial Research, Osaka University, Osaka 567, Japan
(Received 15 October 1997)

We studied the defect physics in $CuInSe_2$, a prototype chalcopyrite semiconductor. We showed that (i) it takes much less energy to form a Cu vacancy in $CuInSe_2$ than to form cation vacancies in II-VI compounds (ii) defect formation energies vary considerably both with the Fermi energy and with the chemical potential of the atomic species, and (iii) the defect pairs such as $(2V_{Cu}^{-}+In_{Cu}^{2+})$ and $(2Cu_{In}^{2-}+In_{Cu}^{2+})$ have particularly low formation energies (under certain conditions, even exothermic). Using (i)–(iii), we (a) explain the existence of unusual ordered compounds $CuIn_5Se_8$, $CuIn_3Se_5$, $Cu_2In_4Se_7$, and $Cu_3In_5Se_9$ as a repeat of a single unit of $(2V_{Cu}^{-}+In_{Cu}^{2+})$ pairs for each $n=4$, 5, 7, and 9 units, respectively, of $CuInSe_2$; (b) attribute the very efficient p-type self-doping ability of $CuInSe_2$ to the exceptionally low formation energy of the shallow defect Cu vacancies; (c) explained in terms of an electronic passivation of the In_{Cu}^{2+} by $2V_{Cu}^{-}$ the electrically benign character of the large defect population in $CuInSe_2$. Our calculation leads to a set of new assignment of the observed defect transition energy levels in the band gap. The calculated level positions agree rather well with available experimental data. [S0163-1829(98)01516-1]

I. INTRODUCTION

$CuInSe_2$ is a prototype member of the family of I-III-VI_2 chalcopyrite semiconductors.[1] The ABX_2 chalcopyrite crystal structure resembles the zinc-blende structure in that each of the two cations A and B are coordinated tetrahedrally by four anions X, but the anion is coordinated by $2A+2B$, with generally dissimilar nearest-neighbor bond lengths $R_{AX} \neq R_{BX}$. The unit cell is thus tetragonal. The electronic structure of bulk chalcopyrite has been studied in some detail, including the calculated band structures, bonding charge densities, and x-ray structure factors,[2] the explanation of why chalcopyrite band gaps are anomalously smaller than in the binary II-VI analogues in terms of p-d repulsion,[3] the analysis and prediction[2,4] of ''bond alternation'' $R_{AX} \neq R_{BX}$, the theory of the order-disorder transition between the ordered chalcopyrite and disordered zinc-blende phases,[5] and the prediction[6] of optical bowing and band offset in chalcopyrite alloys and interfaces, respectively.

To understand the unusual defect physics of this class of materials, it is useful to define their chemical analogues among zinc-blende compounds: In fact, each ternary chalcopyrite has a ''binary II-VI analogue'' derived by taking the ''average cation'' of $A+B$. Thus, ZnX is the binary analogue of CuGaX_2 ($X=$S, Se, and Te) and $Zn_{0.5}Cd_{0.5}X$ is the binary analogue of CuInX_2, etc. The defect physics of $CuInSe_2$ shows three unusual effects with respect to the binary II-VI analogues.

a. Structural tolerance to large off-stoichiometry. Unlike the analogous II-VI pure binaries (ZnSe, CdS), $CuInSe_2$ and other chalcopyrites appear to tolerate a large range of anion-to-cation off stoichiometry (i.e., samples with a few percentage of Cu-poor and/or In-poor stoichiometries are stable[7–9]). The extreme limit of ''off stoichiometry'' is manifested by the existence of a series of compounds with different Cu/In/Se ratios[7–10] ($CuIn_5Se_8$, $CuIn_3Se_5$, $Cu_3In_5Se_9$, etc.), absent in II-VI compounds or their solid solutions such as $Zn_{1-x}Cd_xSe$ or $ZnS_{1-x}Se_x$.

b. The ability to dope $CuInSe_2$ via native defects. Unlike the II-VI analogue, $CuInSe_2$ can be doped n and p type to a low-resistivity level merely via introduction of *native* defects, without extrinsic impurities. Tell, Shay, and Kasper[11] noted that either p- or n-type $CuInSe_2$ crystals could be grown from the melt via stoichiometry control, and Migliorato *et al.*[12] and Noufi *et al.*[13] further investigated this effect, noting that p-type samples can be created by making the sample Cu poor or via anneal in the *maximum* Se pressure, while n-type samples can be made by making the sample Cu rich, or via anneal in *minimum* Se pressure. In contrast, the (small) off stoichiometry attainable in II-VI sulphides and selenides often leads to *deep* levels, inducing in the sample high electrical resistivity. The ability to make p- and n-type $CuInSe_2$ leads to the formation of a p-n homojunction,[14] and eventually to the fabrication of photovoltaic solar cells, reviewed recently in Ref. 15 and in a series of photovoltaics conferences.[16–20]

c. The electrically benign nature of the structural defects. While in Si and in ordinary III-V semiconductors, polycrystallinity leads to a high concentration of electrically active (grain-boundary) defects that have a very detrimental effect on the performance of optoelectronic devices, polycrystalline $CuInSe_2$ is as good an electronic material as its single-crystal counterpart (leading to a $\sim$17% efficient photovoltaic solar cell[21,22]), even though it has many nonstoichiometry defects.

The three puzzling effects regarding the defect structure of $CuInSe_2$ are technologically beneficial: they led, in fact, to the utilization of $CuInSe_2$ in low-cost (i.e., polycrystalline) devices.[15–22] At the same time, these puzzles also led to attempts to understand these unusual phenomena. Yet, despite extensive and successful efforts at *characterization of the*

TABLE I. A comparison of the experimental cohesive energy E_c (Refs. 53 and 54) and Neumann's model calculation of vacancy formation energy $\Delta H_f(V_A)$ (Refs. 51 and 52) in ternaries and the corresponding binaries. The results for $Zn_{0.5}Cd_{0.5}Se$ are an average of ZnSe and CdSe. Note how $\Delta H_f(V_A)$ in the model calculation is proportional to E_c. The present calculation, using appropriate chemical potential do not show such proportionality.

	$CuGaSe_2$	ZnSe	$CuInSe_2$	$Zn_{0.5}Cd_{0.5}Se$
E_c (eV/bond)	1.81	1.32	1.63	1.25
$\Delta H_f(V_A)$ (eV)	3.1–3.4 (A=Cu)	~2.6 (A=Zn)	2.6–3.2 (A=Cu)	~2.6 (A=Zn)

defect levels in $CuInSe_2$ [via electrical measurements,[23–28] absorption,[29–31] luminescence,[12,28,32–40] deep-level transient spectroscopy[41–46] (DLTS) and other means[14,47]], very little evidence exists as to the chemical and structural *identification of the defect centers* producing those levels. One of the main reasons for the failure to reliably identify these defect centers in $CuInSe_2$ is, in our opinion, the methodology used in this process: While native defects in ZnSe were identified through a combination of *structural* and *electronic* characterization experiments (electron paramagnetic resonance, magnetic circular dichromatism, optically-detected nuclear magnetic resonance) with *theoretical* energy-level predictions (see reviews, e.g., in Ref. 48), attempts to identify defect centers in $CuInSe_2$ (Refs. 15, 23, 25, 26, 30, 34–36, and 49–51) followed instead a different route.

(i) First, the formation energies of the leading point defects were estimated[23,25,26,51] from a generalization of the cavity model of Van Vechten (reviewed and revised in Ref. 52), using empirical atomic radii and model bond energies as input. In accordance with the fact that the cohesive (thus, bond) energy of chalcopyrites[53] is larger than that of the binary analogue[54] (Table I), Neumann found indeed larger vacancy formation energies in chalcopyrite relative to II-VIs compounds (Table I).

(ii) It was then assumed that the formation energies are constants, independent of the chemical potentials and Fermi levels. The order of formation energies thus obtained[51] was

$$In_{Cu}<Cu_{In}<V_{Se}<V_{Cu}<V_{In}<Cu_i\,, \tag{1}$$

where V_α denotes a vacancy of atom α, α_i denotes an α-type interstitial, and α_β denotes an antisite of atom α on site β. It was also assumed that the defect abundance follows Eq. (1), i.e., that In_{Cu}, Cu_{In}, V_{Se}, and V_{Cu} are the most abundant defects (in this order). Characterization experiments were then interpreted in light of these expectations, e.g., that In_{Cu} is the main defect.

(iii) It was assumed that only point defects are important; in a few cases,[55] the possible importance of defect complexes (e.g., $In_{Cu}+V_{Cu}$) was mentioned.

With these assumptions it was concluded[30,36] that the 10–30 meV level seen electrically[23–27] and optically[34,35] in In-rich n-type samples is an In_{Cu} shallow donor; that the 60–80 meV level seen in luminescence[12,37,38] both in n-type and p-type materials is[30,36] a V_{Se} donor, that the 20–40 meV level seen in photoluminescence (PL) (Refs. 12, 34, 35, and 38) and electrically[24,25] in n-type materials, or[36] the 160 meV level seen electrically, is[30] a V_{Cu} shallow acceptor, etc.

While the pioneering work of Neumann had contributed a great deal to the understanding of defects in $CuInSe_2$ in the 1980s, it has the serious shortcoming associated with the use of the Van Vechten model. Nowadays, better approach can be followed.[56–59] In the present work we used first-principles self-consistent electronic structure theory to calculate the formation energies and electrical transition levels of point defects *and* defect pairs and arrays in $CuInSe_2$. Our results contradict the previously accepted common practice (i)–(iii) above[23,25,26,51] in identifying point defects in $CuInSe_2$. We find the following.

(i) Due to the monovalent nature of Cu as compared with the divalent Zn, and due to the weaker Cu-Se than Zn-Se covalent bonds, it is much *easier* to form a Cu vacancy in $CuInSe_2$ (i.e., V_{Cu}) than to form a cation vacancy in II-VI compounds. This result is in contrast with the earlier expectation based on the relative cohesive energies of chalcopyrites and zinc-blende compounds (Table I), suggesting that V_{Cu} are more difficult to form (hence, less abundant).

(ii) In accordance with previous first-principles calculations on defect energetics,[56–58,60–64] but in contradiction with Neumann,[23,25,26,51] the defect formation energies are not fixed constants, but vary considerably both with the electronic potential (i.e., the position of the Fermi level), and with the chemical potential of the atomic species. The order of formation energies are (excluding V_{Se})

$$\begin{aligned}
&V_{Cu}<Cu_{In}<V_{In}<Cu_i<In_{Cu} \quad \text{(Cu rich; In rich; } n \text{ type)},\\
&V_{Cu}<Cu_{In}<In_{Cu}<Cu_i<V_{In} \quad \text{(Cu rich; In rich; } p \text{ type)},\\
&V_{Cu}<V_{In}<In_{Cu}<Cu_{In}<Cu_i \quad \text{(Cu poor; In rich; } n \text{ type)},\\
&V_{Cu}<In_{Cu}<V_{In}<Cu_{In}<Cu_i \quad \text{(Cu poor; In rich; } p \text{ type)},\\
&Cu_{In}<V_{In}<V_{Cu}<Cu_i<In_{Cu} \quad \text{(Cu rich; In poor; } n \text{ type)},\\
&Cu_{In}<V_{Cu}<V_{In}<Cu_i<In_{Cu} \quad \text{(Cu rich; In poor; } p \text{ type)},
\end{aligned} \tag{2}$$

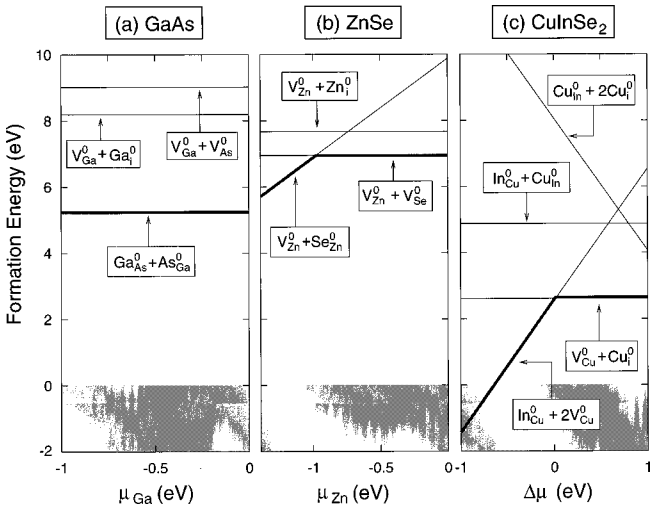

FIG. 1. LDA calculated formation energies of the low-energy, neutral defect pairs in (a) GaAs (Refs. 57 and 63), (b) ZnSe (Ref. 58), and (c) $CuInSe_2$, as a function of the respective atomic chemical potentials. For $CuInSe_2$, $\Delta\mu=(\mu_{Cu}-\mu_{In})/2$ and the plot corresponds to $\mu_s=(\mu_{Cu}+\mu_{In})/2=-1$ (i.e., the BC line in Fig. 2). The shaded area highlights negative formation energies.

to be contrasted with the order of Eq. (1) assumed in all previous analyses of the identity of point defects in $CuInSe_2$.

(iii) Pairing of defects can alter the electric activity. For example, an isolated V_{Cu} is a shallow acceptor, while an isolated In_{Cu} is a deep donor, but a defect pair based on $2V_{Cu}$ and In_{Cu} is electrically inactive.

In addition to challenging the basic assumptions common in the analysis of defects in $CuInSe_2$, we explain puzzles (a)–(c) as follows.

a. Structural tolerance to large off-stoichiometry. The large concentration of off stoichiometry in $CuInSe_2$ is explained here by the unusual stability of $(2V_{Cu}+In_{Cu})$. Figure 1 illustrates that forming this defect take less energy than the corresponding lowest-energy defect pairs in GaAs and ZnSe. The figure shows the calculated formation energies[57,58,63] using the local-density-functional approximation (LDA). We see that in GaAs the lowest-energy defect pair $(Ga^0_{As}+As^0_{Ga})$ requires 5.2 eV to form, while the lowest-energy defect pair in ZnSe, i.e., $(V^0_{Zn}+Se^0_{Zn})$ requires $\sim$6 eV to form. In contrast, in $CuInSe_2$ the formation of $(2V^0_{Cu}+In^0_{Cu})$ at the optimal chemical potential is -1.46 eV. Furthermore, there is a strong interaction between the components of the defect pairs, lowering significantly the pair formation energy. For instance, charging of $(2V^0_{Cu}+In^0_{Cu})$ to form $(2V^-_{Cu}+In^{2+}_{Cu})$ lowers the minimum formation energy from -1.46 to -5.67 eV/pair. Finally, there is also an interaction among different defect pairs in a dense defect array. For example, the interaction between different $(2V^-_{Cu}+In^{2+}_{Cu})$ units is ~ -0.4 eV/pair, thus lowering the formation energy of the periodically repeated arrays to around -6.1 eV/pair. This low formation energy explains the existence of the unusual ''ordered defect compounds'' (ODC's) $CuIn_5Se_8$, $CuIn_3Se_5$, $Cu_2In_4Se_7$, and $Cu_3In_5Se_9$ as a repeat of a single $(2V_{Cu}+In_{Cu})$ unit for each $n=4$, 5, 7, and 9 units, respectively of $CuInSe_2$.

b. The ability to dope $CuInSe_2$ via native defects. The very efficient p-type self-doping ability of $CuInSe_2$ is a consequence of the low formation energy of the Cu vacancies and its very shallow defect level ($\sim$30 meV above the valence-band maximum), as opposed to the *deeper* cation vacancy levels in II-VI compounds.

c. The electrically benign nature of the structural defects. This is explained in terms of the electronic passivation of the In^{2+}_{Cu} deep level by V^-_{Cu}. We find that the $(2V^-_{Cu}+In^{2+}_{Cu})$ pair is electrically neutral and has no *deep* gap levels, and consequently, the ordered defect arrays, e.g., $CuIn_5Se_8$, $CuIn_3Se_5$, and $Cu_3In_7Se_{12}$, all have larger band gaps (1.28, 1.21, and 1.17 eV, respectively) than $CuInSe_2$ (1.04 eV).

II. METHOD OF CALCULATION

A. Calculation of the formation and transition energies

We use the supercell approach in which a defect α in charge state q is placed in an artificially large $CuInSe_2$ cell that is repeated periodically. The defect-defect distance equals the dimension of the supercell. The dimension has thus to be large enough so that the (unphysical) interaction among defects in different cells is negligible and that the position of the Fermi energy E_F (with respect to a reference energy E_i) can be accurately determined.

For a neutral ($q=0$) cation defect (we do not consider Se-related defects in this study) in $CuInSe_2$ the formation energy $\Delta H_f(\alpha,q=0)$ depends on[57,61] the chemical potentials μ:

$$\Delta H_f(\alpha,q=0)=\Delta E(\alpha,q=0)+n_{Cu}\mu_{Cu}+n_{In}\mu_{In}, \quad (3)$$

where

$$\Delta E(\alpha,q=0)=E(\alpha,q=0)-E(CuInSe_2)+n_{Cu}\mu^{solid}_{Cu}+n_{In}\mu^{solid}_{In}. \quad (4)$$

Here, $E(\alpha,q)$ is the total energy of a supercell containing the defect, $E(CuInSe_2)$ is the total energy for the same supercell in the absence of the defect, the n's are the numbers of Cu and In atoms transferred from the supercell to the reservoirs in forming the defect cell, and μ^{solid}_{Cu} and μ^{solid}_{In} are the total energy of ground-state solid Cu (fcc) and solid In (tetragonal).

To calculate the formation energy of charged defects such as V^-_{Cu}, we need to transfer an electron from an electron reservoir and place it on the defect. Thus, the formation energy $\Delta H_f(\alpha,q)$ for a charged defect depends on the absolute Fermi energy E_i+E_F of the electron reservoir. Here E_i is the reference energy and E_F is the Fermi energy relative to the reference. In a supercell calculation, $\Delta H_f(\alpha,q)$ is given by

$$\Delta H_f(\alpha,q)=\Delta H_f(\alpha,q=0)+\delta E(CuInSe_2,-q)+\delta E(\alpha,q)+qE_F. \quad (5)$$

The second term on the right-hand side of Eq. (5) is the difference between the reference energy level of the defect-free $CuInSe_2$ given by the one-particle eigenvalues ϵ_i (e.g., $i=$VBM or CBM, where VBM is valence-band maximum

and CBM is conduction-band minimum) and the energy level determined from total-energy calculations, E_i. Specifically,

$$\delta E(\mathrm{CuInSe_2},-q)=E^{(N+q)}(\mathrm{CuInSe_2})-E^{(N)}(\mathrm{CuInSe_2})$$
$$=-q(\epsilon_i-E_i), \tag{6}$$

Here, $E^{(N)}(\mathrm{CuInSe_2})=E(\mathrm{CuInSe_2})$ is the total energy of the (defect-free) N-electron host. For $q<0$ (i.e., α is an acceptor and usually $i=\mathrm{VBM}$), $E^{(N-|q|)}(\mathrm{CuInSe_2})$ is the total energy of the $CuInSe_2$ with $|q|$ holes in the valence-band maximum (usually at the Γ point) and $|q|$ electron in the reservoir (represented by ''jellium'') having an eigenvalue $\epsilon_{i=\mathrm{VBM}}$. For $q>0$ (i.e., α is a donor and usually $i=\mathrm{CBM}$), $E^{(N+q)}(\mathrm{CuInSe_2})$ is the total energy of the $CuInSe_2$ with q electrons in the CBM and q hole in the reservoir having an eigenvalue $\epsilon_{i=\mathrm{CBM}}$. Notice that, taking the supercell and the jellium reservoir as a whole, $E^{(N+q)}(\mathrm{CuInSe_2})$ is still the total energy of an N-electron system. In a supercell calculation, $\delta E(\mathrm{CuInSe_2},-q)$ is usually small for ordinary semiconductors such as GaAs and ZnSe (~ 0.03 eV), thus is often neglected. However, for semiconductors with localized d character at the VBM, this term can be large. For example, in $CuInSe_2$ $\delta E(\mathrm{CuInSe_2},-1)=0.25$ eV, thus it has to be included in our calculation.

Taking the third term on the right-hand side of Eq. (5),

$$\delta E(\alpha,q)=E^{(M-q)}(\alpha,q)-E^{(M)}(\alpha,q=0). \tag{7}$$

Here, $E^{(M)}(\alpha,q=0)=E(\alpha,q=0)$ is the total energy of the neutral defect with M electrons. $E^{(M-q)}(\alpha,q)$ is the total energy of defect α with $|q|$ electron removed from (for $q>0$) or added to (for $q<0$) the defect level and compensating electrons placed in a reservoir (represented by ''jellium''), having eigenvalue ϵ_i. Notice that, taking the supercell and the jellium background as a whole, we still have an M-electron system. Since in a periodic supercell calculation the potential is determined only up to a constant, we need to make sure that the reference eigenvalues ϵ_i used in the calculations are the same with or without the defects (i.e., fixed with, e.g., vacuum level). This is done by requiring that all of the calculations are performed using the same supercell and same k-point sampling and by lining up the core levels of those atoms that are far away from the defect in the defect cell with the same core levels of the defect-free cell.

The defect transition energy level $\epsilon_\alpha(q/q')$ is defined as the value of the Fermi level where the formation energy of q equals that of q', i.e.,

$$\epsilon_\alpha(q/q')=[\Delta E(\alpha,q)-\Delta E(\alpha,q')]/(q'-q). \tag{8}$$

The formation energy of an ordered defect array is also calculated using Eq. (3). However, in this case, the equilibrium unit-cell volume is determined by total-energy minimization. In contrast, for isolated defects and isolated defect pairs, the unit-cell volume is fixed, equal to that of defect-free $CuInSe_2$.

B. Limits on Fermi energy and atomic chemical potentials

There are some thermodynamic limits to (μ,E_F): E_F is bound between the valence-band maximum (E_V) and the conduction-band minimum (E_C), and $\{\mu_{\mathrm{Cu}},\mu_{\mathrm{In}}\}$ are bound by (i) the values that will cause precipitation of solid elemental Cu, In, and Se, so that

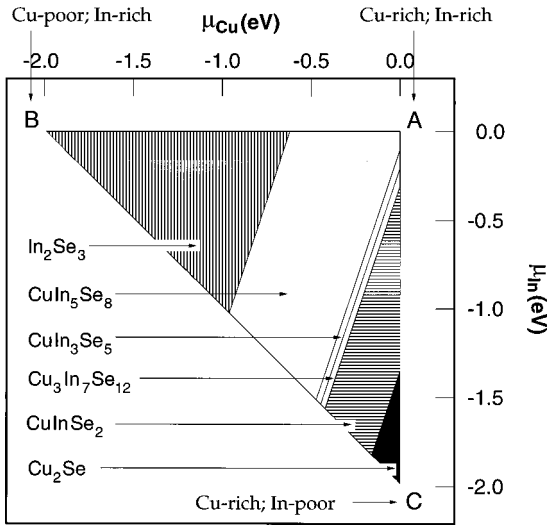

FIG. 2. The calculated stability triangle of the Cu-In-Se systems [Eqs. (9) and (10)] in the $\mu_{\mathrm{Cu}},\mu_{\mathrm{In}}$ plane. The vertices correspond to (A) Cu rich, In rich; (B) Cu poor, In rich, and (C) Cu rich, In poor, respectively.

$$\mu_{\mathrm{Cu}}\leq 0,\quad \mu_{\mathrm{In}}\leq 0,\quad \mu_{\mathrm{Se}}\leq 0; \tag{9}$$

(ii) by the values that maintain a stable $CuInSe_2$ compound, so that

$$\mu_{\mathrm{Cu}}+\mu_{\mathrm{In}}+2\mu_{\mathrm{Se}}=\Delta H_f(\mathrm{CuInSe_2}), \tag{10}$$

where $\Delta H_f(\mathrm{CuInSe_2})=-2.0$ eV is the calculated formation energy of solid $CuInSe_2$, and (iii) by the values that will cause formation of binaries, so that

$$2\mu_{\mathrm{In}}+3\mu_{\mathrm{Se}}\leq\Delta H_f(\mathrm{In_2Se_3}),$$
$$2\mu_{\mathrm{Cu}}+\mu_{\mathrm{Se}}\leq\Delta H_f(\mathrm{Cu_2Se}), \tag{11}$$

where our calculated ΔH_f (tetragonal In_2Se_3)$=-2.1$ eV (Ref. 65) and $\Delta H_f(Cu_2Se)=-0.3$ eV, respectively. Figure 2 gives the calculated ''stability triangle'' in the two-dimensional $(\mu_{\mathrm{Cu}},\mu_{\mathrm{In}})$ plane as defined by Eqs. (9) and (10). The vertices are A (the Cu-rich and In-rich limit), B (the Cu-poor and In-rich limit), and C (the Cu-rich and In-poor limit). Equation (11) defines the regions where In_2Se_3 and Cu_2Se are stable. The stability regions for ordered defect arrays shown inside the triangle of Fig. 2 will be discussed later in Sec. II B.

C. Computational details

We calculated $\Delta H_f(\alpha,q)$ for $\alpha=V_{\mathrm{Cu}}$, V_{In}, $\mathrm{In_{Cu}}$, $\mathrm{Cu_{In}}$, and Cu_i using a supercell approach where a uniform charge density of $\rho=-q/\Omega_{\mathrm{cell}}$ is added to the unit cell of volume Ω_{cell} so that the whole system is charge neutral. We place defect α at the center of a 32-atom tetragonal supercell with lattice vectors $(1,1,0)a$, $(-1,1,0)a$, and $(0,0,2\eta)a$, where

TABLE II. Defect formation energies in term of $\Delta E(\alpha,q)$ in Eq. (3) and defect transition levels $\epsilon_\alpha(q/q')$ of Eq. (8). The n_{Cu} and n_{In} are the numbers of Cu and In atoms and q is the number of excess electrons, transferred from the defect-free crystal to the reservoirs to form one defect.

Defect α	$\Delta E(\alpha,q)$ (eV)	n_{Cu}	n_{In}	q
V_{Cu}^{0}	0.60	$+1$	0	0
V_{Cu}^{-}	0.63			-1
Defect transition level: $(-/0)=E_V+0.03$ eV				
V_{In}^{0}	3.04	0	$+1$	0
V_{In}^{-}	3.21			-1
V_{In}^{2-}	3.62			-2
V_{4n}^{3-}	4.29			-3
Defect transition levels: $(-/0)=E_V+0.17$ eV; $(2-/-)=E_V+0.41$ eV; $(3-/2-)=E_V+0.67$ eV				
$\mathrm{Cu}_{\mathrm{In}}^{0}$	1.54	-1	$+1$	0
$\mathrm{Cu}_{\mathrm{In}}^{-}$	1.83			-1
$\mathrm{Cu}_{\mathrm{In}}^{2-}$	2.41			-2
Defect transition levels: $(-/0)=E_V+0.29$ eV; $(2-/-)=E_V+0.58$ eV				
$\mathrm{In}_{\mathrm{Cu}}^{2+}$	1.85	$+1$	-1	$+2$
$\mathrm{In}_{\mathrm{Cu}}^{+}$	2.55			$+1$
$\mathrm{In}_{\mathrm{Cu}}^{0}$	3.34			0
Defect transition levels: $(0/+)=E_C-0.25$ eV; $(+/2+)=E_C-0.34$ eV				
Cu_i^{+}	2.04	-1	0	$+1$
Cu_i^{0}	2.88			0
Defect transition level: $(0/+)=E_C-0.20$ eV				

$a=5.768$ Å and $\eta=c/a=1.008$ are the calculated lattice constants for $CuInSe_2$. The total energies E in Eq. (5) are calculated using the LDA as implemented by the general potential linearized augmented plane-wave (LAPW) method.[66] The same muffin-tin radius of 2.2 a.u. is used for Cu, In, and Se. The basis set cut-off energy is 10 Ry. We used the Ceperley-Alder exchange correlation potential[67] as parametrized by Perdew and Zunger.[68] The core states are treated relativistically, while the valence states are treated nonrelativistically. In a scalar relativistic or fully relativistic approach, the $CuInSe_2$ band gap is negative. The nonrelativistic direct band gap is 0.17 eV. This LDA band-gap error [the experimental gap is 1.04 eV (Ref. 69)] is corrected by adding a constant energy shift of $1.04-0.17=0.87$ eV to the conduction states so as to match the experimental gap. For isolated defects and defect pairs, we assume that the energy levels of the acceptorlike defects follow the VBM and are thus unchanged while donorlike defect levels follow the CBM and are thus shifted upward by the same amount as the band gap. Defect formation energies were corrected accordingly, e.g., we did not add any correction to the formation energies of the Cu vacancies, but added 0×0.87 eV to $\mathrm{In}_{\mathrm{Cu}}^{2+}$, 1×0.87 eV to $\mathrm{In}_{\mathrm{Cu}}^{+}$, and 2×0.87 eV to $\mathrm{In}_{\mathrm{Cu}}^{0}$, respectively. The Brillouin-zone integration is performed using the equivalent **k** points[70] of the 10 special **k** points in the irreducible zinc-blende Brillouin zone. The atomic positions were fully relaxed for the $q=0$ charge state, but no further relaxation was attempted for $q\neq0$.

The computational error for defect formation energy is estimated as follows: (i) The first source of error is the basis-set cutoff energy of 10 Ry used in the calculation, which introduces an error of <0.03 eV/atom. (ii) The second source of error is the limited accuracy of the LDA in calculating the heats of formation (<0.05 eV/atom). (iii) The third source of error is the unphysical cell-cell interaction in the 32-atom supercell. To estimate it, we assume that the long-range Coulomb interaction among charged defects dominates the cell-cell interaction. Using a dielectric constant of $\epsilon=16$,[69] the cell-cell interaction energy is estimated to be less than ±0.1 eV. (iv) The fourth source of error is the atomic relaxations for $q\neq0$ including the symmetry-breaking Jahn-Teller effect. We did not find any Jahn-Teller effect here, which could be due to the general restriction of the LDA formalism. Otherwise, relaxation for $q\neq0$ is estimated to lower the defect formation energy by less than 0.05 eV. Thus, the total uncertainty in the calculated defect formation energy is less than 0.2 eV. The uncertainty in point defect transition energy levels is ±0.05 eV, and ±0.1 eV for defect pairs. The uncertainty in determining the transition energy levels comes mainly from the difficulty in determining the valence- and conduction-band edges in the defect-containing 32-atom supercell.

III. DEFECT FORMATION ENERGIES

A. Formation energies of isolated point defects

Table II lists the point defect formation energies $\Delta H_f(\alpha,q)$ in terms of $\Delta E(\alpha,q)$, n_{Cu}, n_{In}, and q, as in Eq. (3), and the defect transition energy level $\epsilon_\alpha(q/q')$ [Eq. (8)]. The chemical potential and the Fermi-energy dependence of the defect formation energy depicted in Table II are shown graphically in Figs. 3 and 4, respectively. We see from the figures and Table II the following.

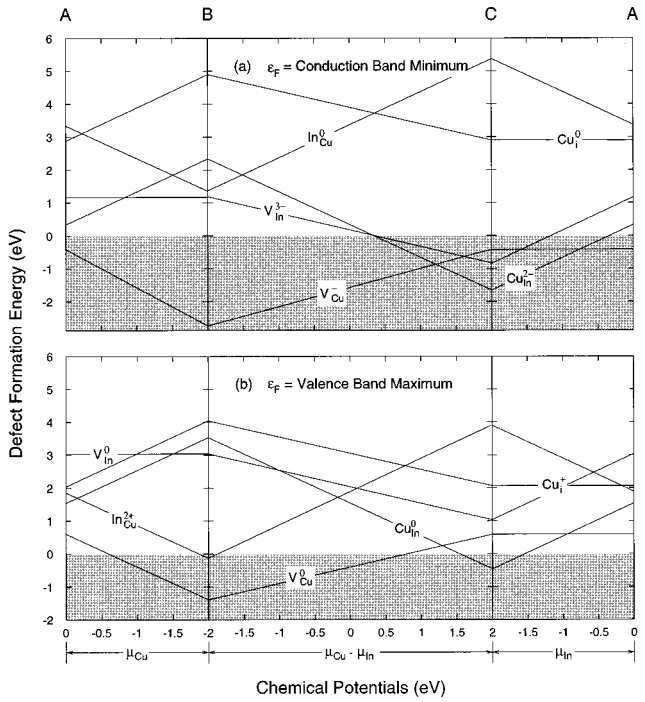

FIG. 3. Formation energies [Eq. (3)] of V_{Cu}, V_{In}, In_{Cu}, Cu_{In}, and Cu_i, as a function of the chemical potentials, μ_{Cu}, $\mu_{Cu}-\mu_{In}$, and μ_{In} with the Fermi energy E_F at the conduction-band minimum (a) and at the valence-band maximum (b). The shaded area highlights negative formation energies.

(i) The relative stability of various defects depends critically on the chemical potentials (see Fig. 3): $\Delta H_f(V_{Cu})$ can vary by as much as 2 eV from point A to B, and $\Delta H_f(Cu_{In})$ can vary by as much as 4 eV from point B to C.

(ii) The formation energies also have a significant dependence on the Fermi energy. In general, as shown in Fig. 4, acceptor states such as V_{Cu}^{-} form more easily in n-type material, while donor states such as In_{Cu}^{2+} form more easily in p-type material. The solid dots in Fig. 4 denote points where the slope of $\Delta H_f(\alpha,q)$ versus q changes; the corresponding value of E_F is the defect transition energy $\epsilon_\alpha(q/q')$ defined in Eq. (8). [Later, in Sec. IV, we will compare the calculated $\epsilon_\alpha(q/q')$ with experiment.]

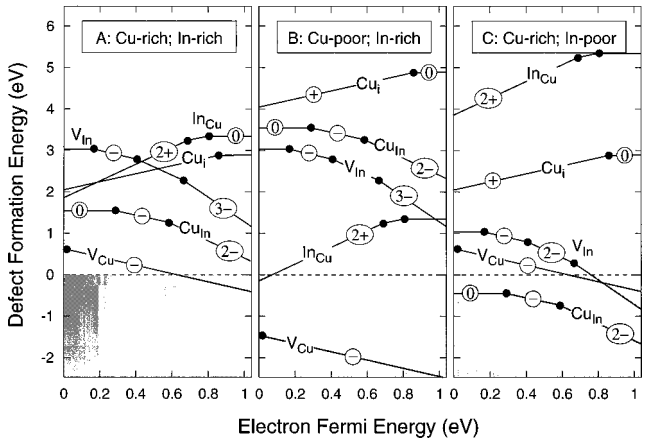

FIG. 4. Formation energies [Eq. (3)] of V_{Cu}, V_{In}, In_{Cu}, Cu_{In}, and Cu_i, as a function of the electron Fermi energy E_F at chemical potentials A, B, and C shown in Fig. 2. Charge state q (in circles) determines the slopes of each line segment. The shaded area highlights negative formation energies. Solid dots denote values of E_F where transition between charge states occurs.

(iii) Some of the formation energies of single neutral defects in $CuInSe_2$ are extraordinary low, e.g., $\Delta H_f(V_{Cu}^0) = -1.4$ eV (at B) and $\Delta H_f(Cu_{In}^0) = -0.5$ eV (at C). In particular, the formation energy of the neutral Cu vacancy is significantly lower than neutral vacancy formation energies for cations in II-VI compounds. Both (a) $E(\alpha,q) - E(CuInSe_2)$ and (b) μ_{Cu}^{solid} in Eq. (3) contribute to the low $\Delta H_f(V_{Cu}^0)$: (a) The low $E(\alpha,q) - E(CuInSe_2)$ has two reasons (''ionic'' and ''covalent''). The ionic reason is that Cu is monovalent, while cations in II-VI compounds are divalent, so the point-ion (Madelung) contribution to the removal energy of the cation is larger in II-VI compounds. The covalent reason is that the Cu-Se bond is easier to break than that of Zn-Se because the Cu $4p$ energy is higher than the Zn $4p$ energy (thus the Cu-Se bond is less covalent). Furthermore, the formation of sp^3 hybrids costs more energy in $CuInSe_2$. This is so because the high-lying Cu $3d$ orbital (relative to the Zn $3d$ orbital) repels the Se $4p$ orbital to higher energy,[71] thus raising the Se $4s \rightarrow 4p$ promotion energy. (b) The low μ_{Cu}^{solid} originates from the fact that solid Cu is more stable [$\mu_{Cu}^{solid} = -E_{cohesive} = -3.49$ eV (Ref. 72)] than either solid In [-2.52 eV (Ref. 72)] or solid Zn [-1.35 eV (Ref. 72)] for V_{Zn} in ZnSe.[73]

(iv) The crucial dependence of ΔH_f on the atomic chemical potentials and the Fermi levels was not addressed in previous calculations[25,26,30,34] and discussions[25,30,51] of defects in $CuInSe_2$. Table III compares our calculated formation energies in terms of the lower bound, the upper bound, the average value, and the range of variation with those of Neumann.[51] We see that besides missing the important variation of ~ 5 eV due to changes in the chemical potentials and Fermi energy, Neumann's results sometimes are also very different from our calculated average values. For example, Neumann's formation energy for the Cu vacancy is about 3.5 eV higher than our calculated average value. This discrepancy is due, in part, to the fact that in Neumann's calculation atomic Cu was used as reference reservoir. As we discussed in Sec. II B, the correct limit of the Cu chemical potential is the solid form of Cu.

B. Formation energies of a defect pair and defect pair arrays

We will discuss association of defects in three steps:

$$\Delta H_f(\alpha+\beta) = \Delta H_{neutral} + \delta H_{int} + \delta H_{ord}. \qquad (12)$$

Here, $\Delta H_{neutral}$ is the formation energy of neutral, noninteracting defects α and β. δH_{int} is the change in energy when α and β are located next to each other to form a defect pair. δH_{ord} is the ordering energy, i.e., the change in energy when the defect pairs form an ordered array.

1. A pair with noninteracting (neutral) constituents: $\Delta H_{neutral}$

Figures 3 and 4 reveal the coexistence of several low-energy point defects of opposite charges at the same E_F and μ. This signals the possibility of association of defects and the formation of charge-compensated defect pairs of low energies. The first three lines of Table IV give, for a few asso-

TABLE III. The lower and upper bounds, the average value, and the range of variation of the calculated point defect formation energies (in eV) in $CuInSe_2$. The corresponding chemical potentials and Fermi energy for the lower and upper bounds are given in parentheses (see Fig. 2 for notations A, B, and C). For comparison, the results of Neumann (Ref. 51) are also shown.

Defect	Lower bound		Upper bound		Average	Range	Neumann
V_{Cu}	−2.41	(B,E_C)	0.63	$(A-C,E_V)$	−0.89	3.04	2.6
V_{In}	−0.83	(C,E_C)	4.29	$(A-B,E_V)$	1.73	5.12	2.8
Cu_{In}	−1.67	(C,E_C)	4.41	(B,E_V)	1.37	6.08	1.5
In_{Cu}	−0.15	(B,E_V)	5.93	(C,E_C)	2.89	6.08	1.4
Cu_i	2.04	$(A-C,E_V)$	5.08	(B,E_C)	3.56	3.04	4.4

ciated defect pairs, the formation energy $\Delta H_{\text{neutral}} = \Delta H_f(\alpha) + \Delta H_f(\beta)$ of neutral, noninteracting defects α and β at the chemical potentials A, B, and C. Notable in Table IV are the low formation energy extrema of the noninteracting vacancy+antisite complexes: $(2V^0_{Cu}+In^0_{Cu})$ of -1.46 eV at B. Also, the neutral antisite pairs $(Cu^0_{In}+In^0_{Cu})$ have a (chemical potential independent) energy of 4.88 eV.

2. A pair with interacting (charged) constituents: δH_{int}

In reality, two defects, located at nearby positions in the crystal, can lower considerably their formation energy through interaction. The interaction includes (a) charge compensation, i.e., transfer of electrons from donor to acceptor levels, (b) subsequent Coulomb attraction between the charge defects, and (c) atomic relaxations driven by, for example, strain relief in case of size mismatch. To find the stable structure of the interacting defect pairs, we consider pair configurations that maximize the point-ion Coulomb interaction and strain relaxation. The final defect pair geometry is obtained by minimizing the quantum-mechanical (LDA) forces on all the atoms inside the unit cell. Figure 5(a) shows the schematic geometry for $(Cu^{2-}_{In}+2Cu^{+}_{i})$ in which two Cu interstitials are collinear with the Cu_{In} antisite. Figure 5(b) shows the schematic geometry for $(2V^{-}_{Cu}+In^{2+}_{Cu})$ where the two Cu vacancies are fcc nearest neighbors of the In_{Cu} antisite and third fcc neighbors between themselves.

The interaction energy made of contributions (a)–(c) noted above δH_{int} is calculated (using the 32-atom supercell) as the difference,

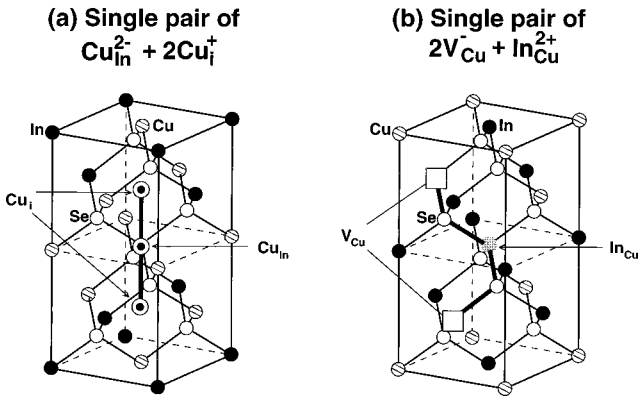

FIG. 5. Calculated minimum Madelung energy configurations of the isolated defect pairs: (a) the $(Cu_{In}+2Cu_i)$ pair and (b) the $(2V_{Cu}+In_{Cu})$ pair. The actual supercell used in our calculation is twice as large as shown here.

$$\delta H_{\text{int}} = \Delta H_f(\alpha^q+\beta^{-q}) - \Delta H_f(\alpha^0) - \Delta H_f(\beta^0), \quad (13)$$

between the cell containing the charged, interacting pair and two cells containing one defect each (thus, noninteracting). Total-energy minimization shows that (fourth line in Table IV) δH_{int} is between -4.2 and -2.0 eV. Note that the energy $\Delta H_{\text{neutral}}+\delta H_{\text{int}}$ of the antisite pair $(Cu^{2-}_{In}+In^{2+}_{Cu})$ dropped to only 0.65 eV, and that this energy for $(2V^{-}_{Cu}+In^{2+}_{Cu})$ is -5.67 eV at B.

We have analyzed the physical origins of δH_{int} by breaking it into the three terms (a)–(c) above: For $(2V^{-}_{Cu}+In^{2+}_{Cu})$, for example, $\delta H_{\text{int}}=-4.21$ eV of which (a) the transfer of two electrons from the high-energy In_{Cu} donor level to low-energy V_{Cu} acceptor level contributes ~ -1.4 eV (this is smaller than twice the band-gap value since In_{Cu} is not a shallow level), (b) a strong electrostatic attraction between the ensuing charged defects contributes, additionally, ~ -2.5 eV, and (c) atomic relaxation upon pairing contributes -0.3 eV.

It is interesting to compare the antisite-pair formation energy of $(Cu^{2-}_{In}+In^{2+}_{Cu})$ in $CuInSe_2$ with that of $(Ga^{2-}_{As}+As^{2+}_{Ga})$ in GaAs. Such antisite pairs are the building blocks of random alloys, e.g., random substitution of Cu and In on cation sites forming a ''zinc-blende'' phase (Cu, In)Se. We find that forming $(Cu^{2-}_{In}+In^{2+}_{Cu})$ in $CuInSe_2$ costs 0.65 eV/pair, whereas forming $(Ga^{2-}_{As}+As^{2+}_{Ga})$ in GaAs costs much higher energy, being 1.8 eV.[57,63] Full randomization of a crystal usually costs much less energy than the formation of a single antisite pair due to pair-pair interaction. It has been shown,[74] for example, that randomization of the GaAs lattice costs only 0.72 eV/pair. For $CuInSe_2$ the randomization energy is only about 0.2 eV/pair.[75] Thus, a disordered ''zinc-blende'' (Cu, In)Se phase is expected to be stable at relatively low temperatures ($\sim$810 °C), unlike GaAs that stays ordered until it melts.

3. Defect pair ordering: δH_{ord}

Defect pairs whose components are charged may order at low temperature in a low-energy configuration to gain the Madelung energy. The formation reaction of the ordered arrays of the $(2V^{-}_{Cu}+In^{2+}_{Cu})$ defect pairs can be written as

$$n(CuInSe_2)+m(In)\rightarrow Cu_{(n-3m)}In_{(n+m)}Se_{2n}+3m(Cu) - \Delta H_f(n,m), \quad (14)$$

where $m=1,2,3,\ldots$ and $n=3,4,5,\ldots$, and where (In) and (Cu) denote In and Cu in their respective equilibrium chemi-

TABLE IV. The calculated formation energies $\Delta H_{\text{neutral}} = \Delta H_f(\alpha) + \Delta H_f(\beta)$ (in eV) of noninteracting *neutral* defects, the intrapair interaction energies δH_{int} and the pair-pair ordering energies $\delta H_{\text{ord}}(n,m=1)$ at chemical potentials A, B, and C shown in Fig. 2.

	$2V_{Cu}^0+In_{Cu}^0$	$Cu_{In}^0+2Cu_i^0$	$V_{Cu}^0+Cu_i^0$	$In_{Cu}^0+Cu_{In}^0$
	4.54(A)	7.30(A)	3.48(A)	4.88(A)
$\Delta H_{\text{neutral}}$	−1.46(B)	13.30(B)	3.48(B)	4.88(B)
	6.54(C)	5.30(C)	3.48(C)	4.88(C)
δH_{int}	−4.21	−4.19	−1.96	−4.23
δH_{ord}	∼−0.43			

cal reservoirs. The search for the minimum-energy configuration (see discussion in Sec. V A below) indicated that atoms on the Cu sublattice form alternative $\cdots$Cu-V_{Cu}-In_{Cu}-V_{Cu}-Cu$\cdots$ planes along the (110) directions. Table IV shows the pair-pair ordering energy $\delta H_{\text{ord}}(n,m)$ for $m=1$ for the most stable structure. We calculate δH_{ord} by subtracting from the LAPW total energy of the defect array the LAPW total energy of isolated interacting $(2V_{Cu}^- + In_{Cu}^{2+})$ pair, i.e.,

$$\delta H_{\text{ord}}(n,m) = \Delta H_f(n,m) - H_f(2V_{Cu}^- + In_{Cu}^{2+}). \qquad (15)$$

$\delta H_{\text{ord}}(n,\ m=1)$ depends weakly on n with an average value of ~ -0.4 eV.

We can see from Table IV that the sum of interaction and ordering energies $\delta H_{\text{int}} + \delta H_{\text{ord}}$ for the defect pair array $(2V_{Cu}^- + In_{Cu}^{2+})$ is about -4.64 eV, which cancels most of the (positive) formation energy of the isolated noninteracting pair: $2\Delta H_f(V_{Cu}^0) + \Delta H_f(In_{Cu}^0) = 4.54$ eV at point A in Fig. 2. Table V shows the formation energies $\Delta H_f(n,\ m=1)$ for a few ordered arrays of $(2V_{Cu}^- + In_{Cu}^{2+})$ for the chemical potentials A, B, and C, respectively. We see that *spontaneous formation of stable defect arrays is predicted*. The horizontal arrows in Fig. 2 point to the chemical potential domains where these ODC's will be thermodynamically stable.

Table VI lists the predicted ODC's that have $\Delta H_f(n,m) < 0$. This list is compared with the observed series of ODC's.[10] We find that the experimental ODC's can be divided into two classes: those that are on the Cu_2Se-In_2Se_3 tie line, i.e., the compounds can be written as $(Cu_2Se)_y(In_2Se_3)_{1-y}$ with $0 \leqslant y \leqslant 1$ (Table VI, fourth column) and those that are not (Table VI, fifth column). We predict the stability of all the In-rich on-tie-line compounds

TABLE V. Calculated formation energies $\Delta H_f(n,m=1) = \Delta H_{\text{neutral}}(\mu) + \delta H_{\text{int}} + \delta H_{\text{ord}}$ of Eq. (12) (in eV) of the ordered arrays of n units of $(2V_{Cu}^- + In_{Cu}^{2+})$ for every m units of $CuInSe_2$. $\delta H_{\text{ord}}(n,m=1)$ are -0.43, -0.45, and -0.46 eV for $n=4$, 5, and 6, respectively, while δH_{int} and $\Delta H_{\text{neutral}}(\mu)$ are taken from the second column of Table IV.

	n	$\mu=A$	$\mu=B$	$\mu=C$
$CuIn_5Se_8$	4	−0.10	−6.10	1.90
$CuIn_3Se_5$	5	−0.12	−6.12	1.88
$Cu_3In_7Se_{12}$	6	−0.13	−6.13	1.87

TABLE VI. Comparison between the predicted ''ordered defect compounds'' made by repeating one unit ($m=1$) of $(2V_{Cu}^- + In_{Cu}^{2+})$ for every n units of $CuInSe_2$ [Eq. (14)] and the observed series of compounds (Ref. 10). The value x is deduced by expressing the ODC in the first column in terms of a $(4CuInSe_2)_x(CuIn_5Se_8)_{1-x}$ alloy.

Predicted			Observed (Ref. 5)	
On tie-line	n	x	On tie-line	Off tie-line
$CuIn_5Se_8$	4	0.00	$CuIn_5Se_8$	
$CuIn_3Se_5$	5	0.20	$CuIn_3Se_5$	
$Cu_3In_7Se_{12}$	6	0.33		$CuIn_7Se_{12}$
$Cu_2In_4Se_7$	7	0.43	$Cu_2In_4Se_7$	
$Cu_5In_9Se_{16}$	8	0.50		$Cu_4In_9Se_{16}$
$Cu_3In_5Se_9$	9	0.56	$Cu_3In_5Se_9$	
$Cu_7In_{11}Se_{20}$	10	0.60		
$Cu_4In_6Se_{11}$	11	0.63		$Cu_3In_6Se_{11}$

as resulting from repetition of m units of $(2V_{Cu}^- + In_{Cu}^{2+})$ in every n units of $CuInSe_2$. These are $CuIn_5Se_8$ ($n=4$, $m=1$), $CuIn_3Se_5$ ($n=5$, $m=1$), $Cu_2In_4Se_7$ ($n=7$, $m=1$), and $Cu_3In_5Se_9$ ($n=9$, $m=1$). In addition, in light of the low formation energy of the neutral Cu vacancy (Figs. 3 and 4), we can rationalize the stabilities of the three observed off-tie-line compounds: $CuIn_7Se_{12}$, $Cu_4In_9Se_{16}$, and $Cu_3In_6Se_{11}$ as emerging from the creation of 2, 1, and 1 Cu vacancies per molecule in the on-tie-line compounds $Cu_3In_7Se_{12}$ ($n=6$, $m=1$), $Cu_5In_9Se_{16}$ ($n=8$, $m=1$), and $Cu_4In_6Se_{11}$ ($n=11$, $m=1$), respectively. Thus, the observed ODC's have a simple explanation in terms of defect physics.

IV. DEFECT TRANSITION ENERGY LEVELS

A. Calculated transition energies

Figure 6 and Table II show the calculated defect transition energy levels $\epsilon_\alpha(q/q')$ of Eq. (8). We see from Fig. 6 that the Cu vacancy has a shallow acceptor level $E(-/0) = E_V + 0.03$ eV, the In vacancy has a somewhat deeper level at $E(-/0) = E_V + 0.17$ eV. All other defect levels are relatively deep, including the two In vacancy acceptor levels at 0.41

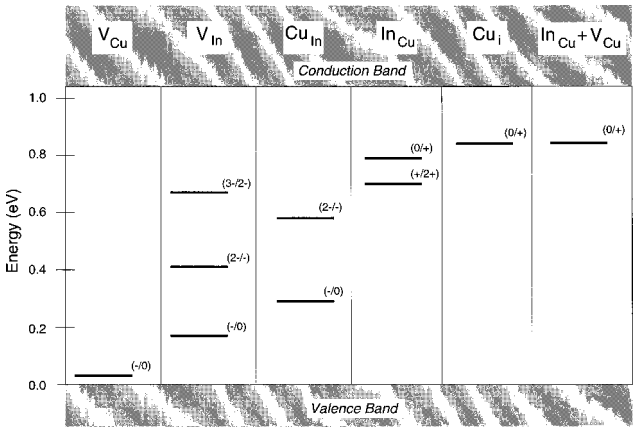

FIG. 6. Calculated defect transition energy levels, corresponding to the filled dots in Fig. 4. These defect levels are defined by Eq. (8) and their exact values are given in Table II. The corresponding charge states for these transitions are given in parentheses.

and 0.67 eV above E_V, respectively. The Cu_{In} antisite also has two deep acceptor levels at 0.29 and 0.58 eV above E_V. The deep donors in $CuInSe_2$ are the In_{Cu} antisite with two levels 0.25 and 0.34 eV, and the Cu interstitial with one level at 0.20 eV below E_C, respectively.

For the isolated interacting $2V_{Cu}^{-}+In_{Cu}^{2+}$ pair, we find that the pairing pushes up the deep In_{Cu} levels to positions much closer to the conduction-band minimum. So the In_{Cu} levels in the pair are no longer harmful electron traps. This, combined with the fact of very low formation energy for this pair, explains the surprising electric tolerance of $CuInSe_2$ to a large amount of structural defects.[69] We also calculated the $(0/+)$ transition energy for $(In_{Cu}+V_{Cu})$ and find that it has a donor level located at $E_C-0.20$ eV.

The calculated Cu vacancy level $E(-/0)=E_V+0.03$ eV is considerably shallower than that of the *isovalent* double acceptor $E(2-/-)=E_V+0.47$ eV of the Zn vacancy in ZnSe. The measured $E(2-/-)$ level of the Zn vacancy[73] is $E_V+0.66$ eV. The difference between the calculated and measured values here may be accounted for by Jahn-Teller distortion not considered in the calculation. One reason for the difference between V_{Cu} and V_{Zn} is that the $E(2-/-)$ level of the Zn vacancy is pushed up by its $E(-/0)$ level. More importantly, however, in $CuInSe_2$ the VBM is pushed considerably higher by the repulsion between Cu $3d$ and Se $4p$ levels[3] than the VBM of ZnSe. Thus, the VBM of the $CuInSe_2$ is much closer to the defect level.

B. Comparison of the calculated and measured transition energies

In Fig. 7, our predicted defect transition levels [Fig. 7(a)] are compared with experimental data [Fig. 7(b)], tabulated in Tables VII and VIII, respectively. Table VII contains the results from various experimental methods including electrical measurements, electrical absorption and photoconductivity, photovoltage, optical absorption, and photoluminescence. These types of measurements in most cases detect, however, only the shallow levels. Table VIII contains, on the other hand, the most recent DLTS measurements on deep levels in $CuInSe_2$. The scattering of the data in Tables VII and VIII is represented in Fig. 7(b) by the width of the histogram, whereas the height of the histogram indicates the number of experiments reporting that defect level. Comparing Figs. 7(a) and 7(b), we see the following.

(i) Our calculated defect levels are in good accord with experiment, especially those of low ionizations, i.e., $(-/0)$ or $(0/+)$. Thus, the calculated $V_{Cu}(-/0)$ acceptor level corresponds to the observed $A1$ level; the $V_{In}(-/0)$ level corresponds to the $A3$ level; the $Cu_{In}(-/0)$ level corresponds to the $A4$ level and the $V_{In}(2-/-)$ level corresponds to the $A5$ level. The $Cu_{In}(2-/-)$ level, within the uncertainty of the calculation, could be the $A6$ level. For donors, both the $Cu_i(0/+)$ and $In_{Cu}(0/+)$ levels may be responsible for the measured $D3$ level, which has a broad range of ~ 90 meV. The $In_{Cu}(+/2+)$ level corresponds to the $D4$ level.

(ii) A number of our assignments of the defect levels are different from those in previous literature, including that (a) the $A1$ level was assigned to V_{In},[25] (b) the $A1$ level was assigned to Cu_{In},[76] and (c) the $D1$ level was assigned to both In_{Cu} (Refs. 39 and 76) and Cu_i.[39] Our calculations do not support these assignments (Fig. 7).

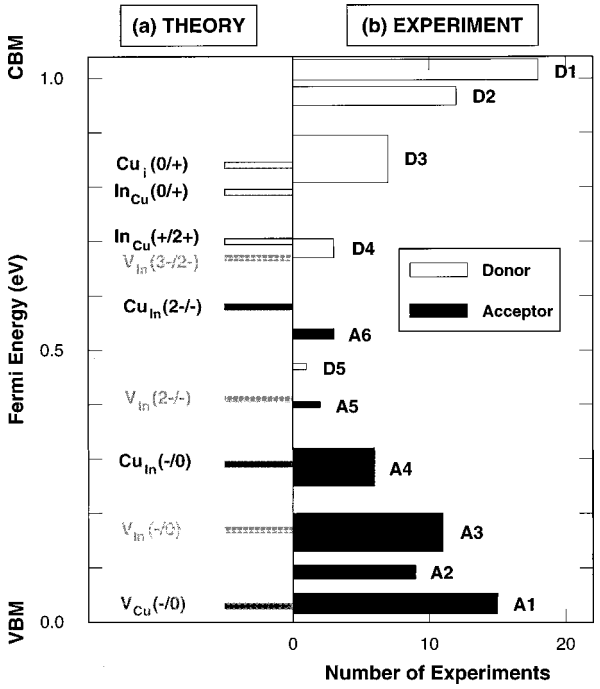

FIG. 7. Defect transition energy levels from (a) the current theory and (b) experiments (taken from Tables VI and VII). The filled bars indicate acceptor levels while the open ones indicate donor levels. In (b), the horizontal axis indicates the number of publications that have made these assignments and the widths of the histograms indicate the spread of the experimental values. A similar histogram plot for experimental data has been given (Ref. 89) earlier by Dagan *et al.*

(iii) The shallow donor levels $D1$ and $D2$ are not assigned from the above calculations. However, it has been speculated that V_{Se} (which was not calculated here) is responsible for the $D1$ level.[30,36] The $D2$ level may be caused by the $(0/+)$ transition of the $(In_{Cu}+V_{Cu})$ pair or by V_{Se} $(+/2+)$. On the other hand, the $A2$ level could be the $(-/0)$ transition of the $(Cu_{In}+Cu_i)$ pair. The uncertainty $(\sim \pm 0.1$ eV) in the current calculation for defect pair energy levels makes it difficult to make a definitive conclusion.

(iv) The calculated $V_{In}(3-/2-)$ level is yet to be assigned experimentally. This level is characterized by its deep position inside the band gap and a high charge state $(3-/2-)$.

V. PROPERTIES OF THE ODC'S

A. Crystal structure of the ODC's

Our search of stable crystal structure of ODC's is guided by the model electrostatic energy calculation and by consideration of the octet rule. We adopt the following rules. (a) Minimum Madelung energy. In calculating Madelung energies, we assume nominal charge, i.e., V_{Cu}, Cu, In, and Se of 0, 1, 3, and -2, respectively. (b) Minimal deviations from the octet rule. There are four cations (including possibly V_{Cu}) on the four vertices of the tetrahedron surrounding each Se atom. To minimize the deviation from the octet rule (eight valence electrons for the four cations), the sum of the cation

TABLE VII. Observed donor and acceptor ionization energies (in meV) for $CuInSe_2$, measured by various means. Data compiled in Ref. 76 are included. Under the column heading ''Method,'' ''Elect.'' denotes electrical measurement, ''Opt. abs.'' denotes optical absorption, PL denotes photoluminescence, PC denotes photoconductivity measurement, and PV denotes photovoltage measurement. Donors (D) are measured with respect to the CBM, while acceptors (A) are given with respect to VBM.

Method	E_{D1}	E_{D2}	E_{D3}	E_{A1}	E_{A2}	E_{A3}	E_{A5}	Ref.
				n-type samples:				
Elect.	10		220					23
Elect.	12		180					24
Elect.	7							25
Elect.	5	80						26
Elect.	6							27
Elect.+PL	35	75	145		105			28
Opt. abs.	6			41				29
Opt. abs.	26	90		54				30
Opt. abs.			232			154		31
PL		70		40				12
PL	35	72			100	150		33
PL	10			33				34
PL	35			45		130		35
PL		60–80		40				38
PC	7		225				400	47
PV	11							14
				p-type samples:				
Elect.				20–28				24
Elect.				35	100		400	25
Opt. abs.			232	38		154		31
PL				40				12
PL					85			32
PL	35	72			100	150		33
PL		55		30	85	130		35
PL		70		40	80			37
PL		60		40	80			38
PL	43			17		162		40
DLTS				16–39	87–92	166–191		46

electrons (denoted as k) should be either 7, 8, or 9. There are therefore only three types of local tetrahedral cationic clusters around each Se: V_{Cu}+Cu+2In ($k=7$), 2Cu+2In ($k=8$), and V_{Cu}+3In ($k=9$). The $k=7$ and $k=9$ clusters must occur in equal numbers to maintain charge neutrality of the overall system. In addition, since the $k=7$ and 9 clusters are oppositely charged, they need to be close to each other to enhance mutual Coulomb attractions.

Using these rules, any ''on-tie-line ODC'' (Table VI) represents a weighted distribution of the three clusters. For examples, $CuInSe_2$ in the chalcopyrite structure consists of 100% of the $k=8$ clusters; $CuIn_5Se_8$ consists of 50% of the $k=7$ and 50% of the $k=9$ clusters; $CuIn_3Se_5$ has 20% of the $k=8$ cluster and 40% each of the $k=7$ and $k=9$ clusters, etc.

Following the rule above, we find that for stoichiometric $CuInSe_2$ the chalcopyrite structure [Fig. 8(a)] has the lowest energy, while for $CuIn_5Se_8$, the lowest-energy order defect compounds has the structure shown in Fig. 8(b). This structure can be obtained from chalcopyrite $CuInSe_2$ by having one ($2V_{Cu}+In_{Cu}$) defect pair in every 16-atom $Cu_4In_4Se_8$ unit cell. In this case, the In and Se sublattices are unperturbed while atoms on the Cu sublattice form alternative $\cdots$Cu-V_{Cu}-In_{Cu}-V_{Cu}-Cu$\cdots$ planes along the [110] direction. Our first-principles total-energy calculations confirmed that these are indeed the lowest-energy structures.[77] However, we also find that as long as two crystal structures have the same local environment (i.e., the same type of tetrahedral clusters) the energy difference between the two structures will be very small.[77] For example, $CuInSe_2$ in the CuAu structure has only the $k=8$ tetrahedral clusters, same as the $CuInSe_2$ in the chalcopyrite structure. We find that its total energy is only slightly higher ($\sim$2 meV/atom) than the chalcopyrite structure. The LDA calculations here do not involve any approximations used for isolated defects and defect pairs (Sec. II C) and are thus accurate to within 0.5 meV/atom. Similarly, the LDA ordering energy of ODC's (see below) are also more accurate than the energy of isolated defects.

The calculated lattice constant of $CuIn_5Se_8$ is 5.715 Å, which is about 1% smaller than the calculated lattice constant of $CuInSe_2$. We find that in this ODC structure the Cu-Se and In-Se bond lengths are similar to their ideal val-

TABLE VIII. Deep donor and acceptor ionization energies (in meV) for $CuInSe_2$, measured by DLTS on Schottky junctions and/or homojunctions. The defect concentrations, if reported, are rather low, in the range of 10^{12}–10^{14} cm^{-3}. Donors (D) and acceptors (A) are given with respect to the CBM and VBM, respectively.

Type	E_{D3}	E_{D4}	E_{D5}	E_{A3}	E_{A4}	E_{A6}	Ref
n		370					41
n	182	335					43
n		350	570				44
p				200		540	41
p					280,320		41
?					250	520	42
?				120–190	260–280		45
p				186	250	520	43
p					220–280		44
p				166–191	276		46

ues in $CuInSe_2$, while the Se-V_{Cu} distance is about 10% shorter than the Se-Cu bond length.

To aid in experimental identification of this crystal structure, Table IX gives our calculated static x-ray structure factors $|\rho(\mathbf{G})|$) of ground-state $CuInSe_2$ and $CuIn_5Se_8$ (Fig. 8), respectively. The structure factors $\rho(\mathbf{G})$ are Fourier transform of the electron charge density $n(\mathbf{r})$, i.e.,

$$\rho(\mathbf{G}) = \frac{1}{\Omega} \int_{\Omega} n(\mathbf{r}) e^{i\mathbf{G}\cdot\mathbf{r}} d\mathbf{r}. \tag{16}$$

Here $\mathbf{G}$ is the reciprocal lattice vector and Ω is the unit-cell volume. Experimental diffraction intensity is proportional to $|\rho(\mathbf{G})|^2$ and associated Debye-Waller factors.[78] To find $\rho(\mathbf{G})$ for other ODC's that can be expressed as a $(4CuInSe_2)_x(CuIn_5Se_8)_{1-x}$ alloy (see Table VI), we can use the approximation that the structure factors of these ODC's for the $\mathbf{G}$ vectors given in Table IX are the weighted averages of the structure factors of $CuInSe_2$ and $CuIn_5Se_8$.

The calculated structure factors for $CuIn_5Se_8$ (Table IX) contain a ($\frac{1}{2}$ $\frac{1}{2}$ 0) spot, signaling the formation of the (110) $\cdots$Cu-V_{Cu}-In_{Cu}-V_{Cu}-Cu$\cdots$ superlattice. It also has a strong (001) spot reflecting the existence of the (001) vacancy planes. Since $CuIn_3Se_5$ can be viewed as a superposition of

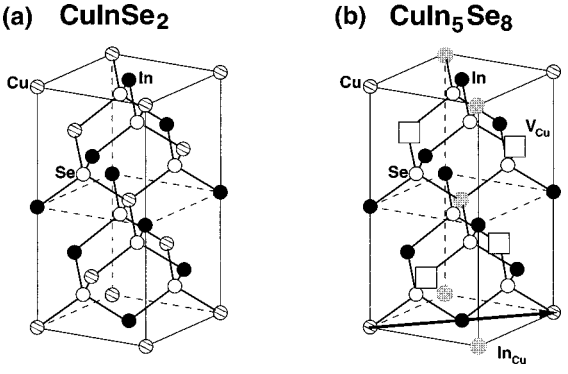

FIG. 8. Crystal structure of (a) chalcopyrite $CuInSe_2$ and (b) the ground state $CuIn_5Se_8$. Structure (b) can be derived by forming defect chain $\cdots$Cu-V_{Cu}-In_{Cu}-V_{Cu}-Cu$\cdots$ in the Cu sublattice of structure (a) along the [110] direction.

TABLE IX. Calculated magnitude of structure factors $|\rho(\mathbf{G})|$ [Eq. (16)] (in electron per chalcopyrite cell) of $CuInSe_2$ and $CuIn_5Se_8$. Here, $\mathbf{G}$ is the reciprocal lattice vector, in units of $2\pi/a$ ($2\pi/\eta a$ for the c axis), where a and $\eta \sim 1$ are the tetragonal lattice parameters. Due to the symmetry $|\rho(\mathbf{G})| = |\rho(-\mathbf{G})|$ and are the same for all $\mathbf{G}$ vectors in a star.

$\mathbf{G}$	$CuInSe_2$ $\lvert\rho(\mathbf{G})\rvert$	$CuIn_5Se_8$ $\lvert\rho(\mathbf{G})\rvert$
0,0,0	292	273
$\frac{1}{2},\frac{1}{2},0$		5.04
$\frac{1}{2},\bar{\frac{1}{2}},\frac{1}{2}$		4.66
0,0,1	0.00	20.36
$1,0,\frac{1}{2}$	13.05	27.75
$0,1,\frac{1}{2}$	13.05	27.58
$\frac{1}{2},\frac{1}{2},1$		4.00
1,1,0	0.00	30.98
1,1,0	0.00	30.93
$\frac{3}{2},\bar{\frac{1}{2}},0$		15.90
$\frac{1}{2},\bar{\frac{3}{2}},0$		2.13
$\frac{1}{2},\bar{\frac{1}{2}},\bar{\frac{3}{2}}$		9.36
$\frac{3}{2},\frac{1}{2},\bar{\frac{1}{2}}$		8.46
$\frac{1}{2},\frac{3}{2},\bar{\frac{1}{2}}$		14.55
1,1,1	177.51	162.22
1,1,1	177.51	162.76
$1,0,\bar{\frac{3}{2}}$	36.08	54.90
$0,1,\bar{\frac{3}{2}}$	36.08	54.56

80% $CuIn_5Se_8$ and 20% $CuInSe_2$, the above features should be carried over to $CuIn_3Se_5$. Electron diffraction observed by Xiao, Yang, and Rockett[79] indeed suggests that Cu vacancies form (001) planes in $CuIn_3Se_5$.

There are already a number of x-ray studies of the ordered defect compounds, from which several structure models have been proposed to describe the ODC.[80–87] Our calculations[77] suggest that at a given Cu/In ratio, many ODC polytypes with the same local environment have nearly degenerate total energy (within 8 meV/atom), growth kinetics, and history of annealing, and the configuration entropies are likely to control the final structure of the ODC's.

B. Electronic structure of the ODC's

To further aid in experimental characterization of the ODC's, we calculated their band structures and band offsets. We corrected the LDA band gaps for all the ODC's by the value of stoichiometric $CuInSe_2$ (0.87 eV). We find that for $CuIn_5Se_8$, $CuIn_3Se_5$ and $Cu_3In_7Se_{12}$ the LDA-corrected band gaps are 1.34, 1.26, and 1.21 eV, respectively, all larger than the 1.04-eV gap of $CuInSe_2$. The increase in the band gap of the ordered defect compounds is caused by a reduced Se p-Cu d interband repulsion due to the diminished d character attendant upon forming dense, periodic Cu vacancies. This lowers the VBM of $CuIn_5Se_8$.

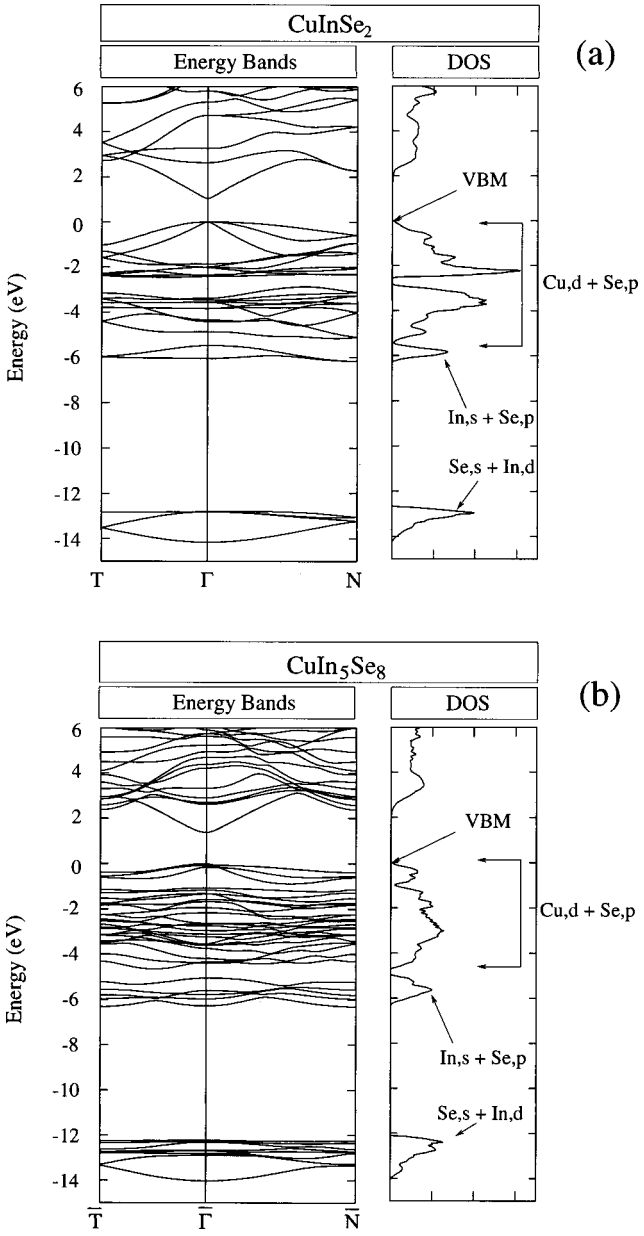

FIG. 9. Calculated band structure and density of states for (a) $CuInSe_2$ and (b) $CuIn_5Se_8$. The energy zero is at the VBM. The features of the density of states are identified according to their main atomic characters. Notice the p-d repulsion gap at VBM~ -2.5 eV in $CuInSe_2$.

Figure 9 shows our calculated band structure and density of states (DOS) of $CuInSe_2$ (a) and $CuIn_5Se_8$ (b). The features in the DOS are identified according to their main atomic characters. For $CuInSe_2$ [Fig. 9(a)], we see that (i) the bottom of the valence band (at VBM~ -13 eV) consists of mostly Se 4s orbitals, hybridized with the In 4d semicore states below (not shown), (ii) the bottom of the upper valence band (at $\sim$VBM-6 eV) has the bonding In s and Se p characters, (iii) the largest peak at VBM$-\sim -2$ eV is due to the nonbonding Cu $d(e_2)$ states, and (iv) most of the upper valence bands (0–5 eV below the VBM) consists of the hybridized Cu d and Se p characters. The p-d repulsion is very large in $CuInSe_2$ that a p-d repulsion gap of 0.2 eV is formed at VBM~ -2.5 eV [Fig. 9(a)], which separate the bonding p-d states below and the antibonding p-d states above. This analysis is substantiated by an inspection of the calculated charge density of the VBM state show in Fig. 10(a). It indicates that for $CuInSe_2$, the VBM is an *antibonding* Cu d and Se p state with a node along the Cu-Se bond.

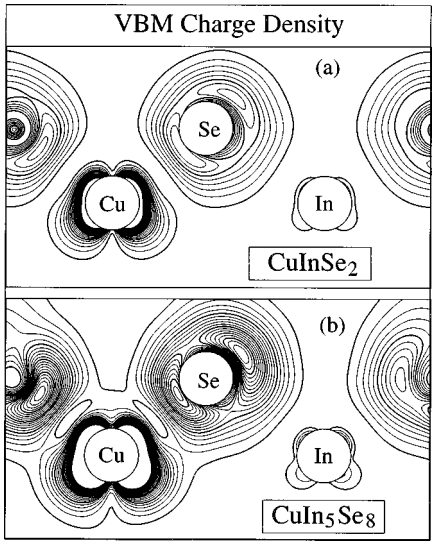

FIG. 10. Contour plot of the calculated charge density of the VBM states for (a) $CuInSe_2$ and (b) $CuIn_5Se_8$.

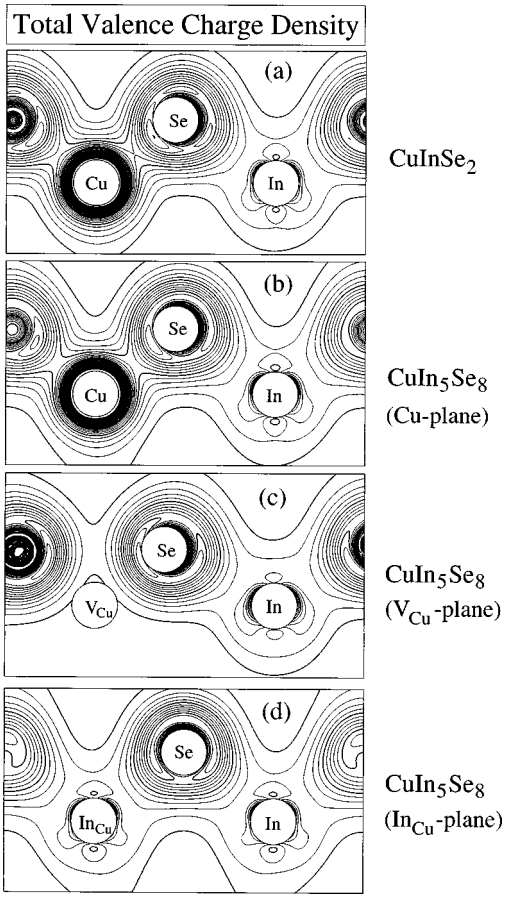

FIG. 11. Contour plot of the calculated total valence charge density for (a) $CuInSe_2$ and (b)–(d) $CuIn_5Se_8$. For $CuIn_5Se_8$, the respective results of three atomic planes passing the Cu atom (b), the Cu vacancy (c) and the In-on-Cu antisite (d), are shown.

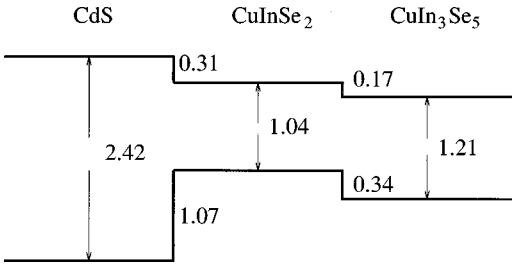

FIG. 12. Calculated band offsets (in eV) between CdS, $CuInSe_2$, and $CuIn_3Se_5$.

For $CuIn_5Se_8$ the main character of its DOS [Fig. 9(b)] are similar to that for $CuInSe_2$ [Fig. 9(a)], except that the peaks are broadened. The major differences occur at the upper valence bands. In $CuIn_5Se_8$ three Cu atoms in each unit cell are replaced by two V_{Cu} and one In_{Cu}, thus, the p-d hybridization (repulsion) is much weaker in $CuIn_5Se_8$ than in $CuInSe_2$. This weaker p-d repulsion lowers the VBM and diminishes the p-d repulsion gap observed in $CuInSe_2$. The charge density of the VBM state in $CuIn_5Se_8$ [Fig. 10(b)] also shows stronger *bonding* character along the Cu-Se bond than that in $CuInSe_2$ [Fig. 10(a)].

Figure 11 depicts the total valence charge density for $CuIn_5Se_8$ in three atomic planes passing the Cu atom (b), the Cu vacancy (c) and the In-on-Cu antisite (d), compared with that of $CuInSe_2$ (d). It shows that after the formation of the $(2V_{Cu}+In_{Cu})$ defect array, the *change* of the bonding charge surrounding the Se atom is small. This is consistent with the small formation energy of $CuIn_5Se_8$.

Finally, using a procedure analogous[6] to the one employed in the photoemission core-level spectroscopy, we have calculated the band alignment between $CuInSe_2$ and $CuIn_5Se_8$ (see the structures in Fig. 8). We find that the unstrained VBM of $CuIn_5Se_8$ is 0.42 eV lower than that of $CuInSe_2$, while the CBM of $CuIn_5Se_8$ is 0.18 eV lower than that of $CuInSe_2$. This lowering of the CBM of $CuIn_5Se_8$ is due to a combined effect of the Cu vacancies and In_{Cu} antisites. It is relatively small because the effective electrostatic potentials of the vacancies and antisites have opposite signs, thus canceling each other. Band alignment between other ODC's and $CuInSe_2$ can be obtained by interpolation of the values between $CuInSe_2$ and $CuIn_5Se_8$. We find that, for $CuIn_3Se_5$ ($x=0.2$, see Table VI), its VBM and CBM are 0.34 and 0.17 eV lower than $CuInSe_2$, respectively. This results are depicted in Fig. 12. Our predictions are in good agreement with the recent measurement of Schock and Stolt,[88] who found the the valence- and conduction-band offsets between $CuInSe_2$ and $CuIn_3Se_5$ are 0.28 and 0.02 eV, respectively. We noticed that the actual band offset depend on the $CuIn_3Se_5$ crystal structure realized in the experiment.[77]

VI. SUMMARY

We summarize our results as follows: (i) it is much easier to form neutral Cu vacancy in $CuInSe_2$ than cation vacancy in II-VI compounds. (ii) Defect formation energies are not fixed constants, but vary considerably with both the electronic potential and with the chemical potential of the atomic species. Negative defect formation energies are thus possible at optimal chemical potentials. (iii) Defect pairs are abundant, and can alter significantly the electric activity in the sample. Based on (i)–(iii), we explained (a) the existence of the off-stoichiometric ordered compounds, as a repeat of m units of $(2V_{Cu}^{-}+In_{Cu}^{2+})$ pairs for each n units of $CuInSe_2$. (b) We attribute the very efficient self-doping ability of $CuInSe_2$ to the exceptionally low formation energy of Cu vacancies and to the existence of a *shallow* Cu vacancy acceptor level. (c) The electrically benign character of the large defect population in $CuInSe_2$ is explained in terms of an electronic passivation of the In_{Cu}^{2+} by $2V_{Cu}^{-}$. With new assignments for several key defect levels, the calculated defect transition energy levels appear to agree rather well with available experimental data.

ACKNOWLEDGMENTS

We thank Dr. D. Cahen for a critical reading of the manuscript. This work was supported by the U.S. DOE-EE, under Contract No. DE-AC36-83CH10093.

[1] J. L. Shay and J. H. Wernick, *Ternary Chalcopyrite Semiconductors* (Pergamon, Oxford, 1975).
[2] J. E. Jaffe and A. Zunger, Phys. Rev. B **28**, 5822 (1983); **30**, 741 (1984).
[3] J. E. Jaffe and A. Zunger, Phys. Rev. B **27**, 5176 (1983); **29**, 1882 (1984).
[4] J. L. Martins and A. Zunger, Phys. Rev. B **32**, 2689 (1984).
[5] A. Zunger, Appl. Phys. Lett. **50**, 164 (1987); S.-H. Wei, L. G. Ferreira, and A. Zunger, Phys. Rev. B **45**, 2533 (1992); R. Osorio, Z. W. Lu, S.-H. Wei, and A. Zunger, Phys. Rev. B **47**, 9985 (1993).
[6] S.-H. Wei and A. Zunger, J. Appl. Phys. **78**, 3846 (1995); Appl. Phys. Lett. **63**, 2549 (1993).
[7] L. S. Palatnik and E. I. Rogacheva, Dokl. Akad. Nauk SSSR **174**, 80 (1967).
[8] M. L. Fearheiley, Sol. Cells **16**, 91 (1986).
[9] K. J. Bachmann, M. Fearheiley, Y. H. Shing, and N. Tan, Appl. Phys. Lett. **44**, 407 (1989).
[10] P. Villars and L. D. Calvert, *Pearson's Handbook of Crystallographic Data for Intermetallic Phases* (ASM International, Materials Park, Ohio, 1991), p. 2884, and references therein.
[11] B. Tell, J. L. Shay, and H. M. Kasper, J. Appl. Phys. **43**, 2469 (1972).
[12] P. Migliorato, J. L. Shay, H. M. Kasper, and S. Wagner, J. Appl. Phys. **46**, 1777 (1975).
[13] R. Noufi, R. Axton, C. Herrington, and S. K. Deb, Appl. Phys. Lett. **45**, 668 (1984).
[14] J. Parkes, R. D. Thomlinson, and M. J. Hampshiere, Solid-State Electron. **16**, 773 (1973).
[15] A. Rockett and E. W. Birkmire, J. Appl. Phys. **70**, R81 (1991).
[16] *The Conference Record of the Twenty-fifth IEEE Photovoltaic Specialists Conference* (IEEE, New York, 1996).

[17] *The Conference Record of the Twenty-third IEEE Photovoltaic Specialists Conference* (IEEE, New York, 1994).
[18] *The Conference Record of the Twenty-second IEEE Photovoltaic Specialists Conference* (IEEE, New York, 1993).
[19] *The Conference Record of the Twenty-first IEEE Photovoltaic Specialists Conference* (IEEE, New York, 1991).
[20] *The Conference Record of the Twentieth IEEE Photovoltaic Specialists Conference* (IEEE, New York, 1990).
[21] J. Hedstrom, H. J. Olsen, M. Bodegard, A. Kylner, L. Stolt, D. Hariskos, M. Ruckh, and H. W. Schock, *The Conference Record of the Twenty-third IEEE Photovoltaic Specialists Conference* (IEEE, New York, 1993), p. 364.
[22] A. M. Gabor, J. R. Tuttle, D. S. Albin, M. A. Contreras, R. Noufi, and A. M. Hermann, Appl. Phys. Lett. **65**, 198 (1994).
[23] H. Neumann, N. Van Nam, H. Hobler, and G. Kuhn, Solid State Commun. **25**, 899 (1978).
[24] T. Irie, S. Endo, and S. Kimura, Jpn. J. Appl. Phys. **18**, 1303 (1979).
[25] H. Neumann, E. Nowak, and G. Kuhn, Cryst. Res. Technol. **16**, 1369 (1981); H. Neumann, *ibid.* **18**, 483 (1983); **18**, 901 (1983).
[26] H. Neumann, R. D. Tomlinson, N. Avgerinos, and E. Nowak, Phys. Status Solidi A **75**, K199 (1983).
[27] S. M. Wasim and A. Noguera, Phys. Status Solidi A **82**, 553 (1984).
[28] H. Y. Ueng and H. L. Hwang, J. Phys. Chem. Solids **50**, 1297 (1989).
[29] C. Rincon and J. Gonzalez, Phys. Status Solidi B **110**, K171 (1982).
[30] C. Rincon and C. Bellabarba, Phys. Rev. B **33**, 7160 (1986); S. M. Wasim, Sol. Cells **16**, 289 (1986).
[31] A. Zegadi, D. M. Bagnall, A. E. Hill, M. A. Slifkin, H. Neumann, and R. D. Tomlinson, in *Twelfth European Photovoltaic Solar Energy Conference: Proceedings of the International Conference*, edited by R. Hill, W. Palz, and P. Helm (H. S. Stephens & Associates, Bedford, 1994), p. 1576.
[32] P. W. Yu, Solid State Commun. **18**, 395 (1976).
[33] J. J. M. Binsma, L. J. Giling, and J. Bloem, J. Lumin. **27**, 35 (1982).
[34] C. Rincon, J. Gonzalez, and G. Sunchez-Perez, J. Appl. Phys. **54**, 6634 (1983); Sol. Cells **16**, 335 (1986).
[35] F. Abou-Elfotouh, D. J. Dunlavy, D. Cahen, R. Noufi, L. L. Kazmerski, and K. J. Bachmann, Prog. Cryst. Growth Charact. **10**, 365 (1985).
[36] R. E. Hollingsworth and J. R. Sites, *The Conference Record of the Eighteenth IEEE Photovoltaic Specialists Conference* (IEEE, New York, 1985), p. 1409.
[37] P. Lange, H. Neff, M. Fearheiley, and K. J. Bachmann, Phys. Rev. B **31**, 4074 (1985).
[38] G. Masse' and E. Redjai, J. Phys. Chem. Solids **47**, 99 (1986); J. Appl. Phys. **56**, 1154 (1984).
[39] F. Abou-Elfotouh, H. Moutinho, A. Bakry, T. J. Coutts and L. L. Kazmerski, Sol. Cells **30**, 151 (1991).
[40] W. Z. Shen, S. C. Shen, Y. Chang, W. G. Tang, L. S. Yip, W. W. Lam, I. Shih, Infrared Phys. Technol. **37**, 509 (1996).
[41] H. J. Moller and E. M. Rodak, in *Tenth E.C. Photovoltaic Solar Energy Conference: Proceedings of the International Conference*, edited by A. Luque *et al.* (Kluwer Academic, Boston, 1991), p. 913.
[42] L. S. Yip, W. S. Weng, L. Li, I. Shih, and C. H. Champness, in *Tenth E.C. Photovoltaic Solar Energy Conference: Proceedings of the International Conference*, edited by A. Luque *et al.* (Kluwer Academic, Boston, 1991), p. 921.
[43] A. Li and J. Shih, J. Electron. Mater. **22**, 195 (1993).
[44] M. Igalson and R. Bacewicz, in *Twelfth European Photovoltaic Solar Energy Conference: Proceedings of the International Conference*, edited by R. Hill, W. Palz, and P. Helm (H. S. Stephens & Associates, Bedford, 1994), p. 1584.
[45] M. Schmitt, U. Rau and J. Parisi, in *Thirteenth European Photovoltaic Solar Energy Conference: Proceedings of the International Conference*, edited by W. Freiesleben *et al.* (H.S. Stephens & Associates, Bedford, 1995), p. 1969.
[46] A. M. Bakry and A. M. Elnaggar, J. Mater. Sci. Mater. Electron. **7**, 191 (1996).
[47] H. Sobotta, H. Neumann, V. Riede, G. Kuhn, J. Seltmann, and D. Oppermann, Phys. Status Solidi A **60**, 531 (1980).
[48] G. D. Watkins, J. Cryst. Growth **159**, 338 (1996); G. D. Watkins, in *Defect Control in Semiconductors*, edited by K. Sumino (Elsevier, Amsterdam, 1990), p. 933.
[49] L. Roa, C. Rincon, J. Gonzales, and M. Quintero, J. Phys. Chem. Solids **51**, 551 (1990).
[50] D. Cahen in *Ternary and Multinary Compounds*, edited by S. Deb and A. Zunger (Materials Research Society, Pittsburgh, 1987), p. 433.
[51] The full results were not published by H. Neumann, but were reproduced by C. Rincon and C. Bellabarba via private communication (Ref. 30). These values appear different in some cases than those given by H. Neumann, Cryst. Res. Technol. **18**, 901 (1983).
[52] J. A. Van Vechten, in *Handbook of Semiconductors*, edited by S. P. Keller (North Holland, Amsterdam, 1980), Vol. 3, p. 1.
[53] D. Cahen and R. Noufi, J. Phys. Chem. Solids **53**, 991 (1992).
[54] *Semiconductors. Physics of II-VI and I-VII Compounds*, edited by O. Madelung, M. Schulz, and H. Weiss, Landolt-Börnstein, New Series, Group III, Vol. 17, Pt. b (Springer, Berlin, 1982).
[55] D. Cahen, D. Abecassis, and D. Soltz, Chem. Mater. **1**, 202 (1989).
[56] G. A. Baraff and M. Schluter, Phys. Rev. Lett. **55**, 1327 (1985).
[57] S. B. Zhang and J. E. Northrup, Phys. Rev. Lett. **67**, 2339 (1991).
[58] D. B. Laks, C. G. Van de Walle, G. F. Neumark, P. E. Bloche, and S. T. Pantelides, Phys. Rev. B **45**, 10 965 (1992) and C. Van De Walle (private communication).
[59] M. A. Berding, M. van Schifgaarde, and A. Sher, J. Vac. Sci. Technol. B **10**, 1471 (1992).
[60] G. A. Baraff and M. Schluter, Phys. Rev. B **33**, 7346 (1986).
[61] A. Zunger in *Solid State Physics*, edited by F. Seitz and D. Turnbul (Academic, New York, 1986), Vol. 36, p. 275.
[62] R. W. Jansen and O. F. Sankey, Phys. Rev. B **39**, 3192 (1989).
[63] J. E. Northrup and S. B. Zhang, Phys. Rev. B **47**, 6791 (1993).
[64] J. E. Northrup and S. B. Zhang, Phys. Rev. B **50**, 4962 (1994).
[65] The calculated formation enthalpy of In_2Se_3 of the hexagonal structure is about 1.1 eV lower than that of the cubic structure. We will not, however, consider the hexagonal structure here since there is a macroscopic transformation energy barrier between the two. Experimentally, Cu-In-Se compounds are cubic (or tetragonal) as long as they are grown from cubic $CuInSe_2$ or via epitaxial growth on a zinc-blende substrate (Refs. 9, 10 and 87).
[66] S.-H. Wei and H. Krakauer, Phys. Rev. Lett. **55**, 1200 (1985); D. J. Singh, *Planewaves, Pseudopotentials, and the LAPW Method* (Kluwer, Boston, 1994).
[67] D. M. Ceperly and B. J. Alder, Phys. Rev. Lett. **45**, 566 (1980).
[68] J. P. Perdew and A. Zunger, Phys. Rev. B **23**, 5048 (1981).

[69] *Copper Indium Diselenide for Photovoltaic Applications*, edited by T. J. Coutts, L. L. Kazmerski, and S. Wagner (Elsevier, Amsterdam, 1986).
[70] S. Froyen, Phys. Rev. B **39**, 3168 (1989).
[71] S.-H. Wei and A. Zunger, Phys. Rev. B **37**, 8958 (1988).
[72] C. Kittel, *Introduction to Solid State Physics*, 6th ed. (Wiley, Singapore, 1986), p. 55.
[73] D. Y. Jeon, H. P. Gislason, and G. D. Watkins, Phys. Rev. B **48**, 78 72 (1993).
[74] D. B. Laks, R. Magri, and A. Zunger, Solid State Commun. **83**, 21 (1992).
[75] S.-H. Wei and A. Zunger, Phys. Rev. B **45**, 2533 (1992).
[76] C. Rincon and S. M. Wasim, in *Ternary and Multinary Compounds*, edited by S. K. Deb and A. Zunger (Materials Research Society, Pittsburgh, PA, 1987), p. 443.
[77] S.-H. Wei, S. B. Zhang, and A. Zunger (unpublished).
[78] Z. W. Lu, A. Zunger, and M. Deutsch, Phys. Rev. B **47**, 9385 (1993).
[79] H. Z. Xiao, L.-Chung Yang, and A. Rockett, J. Appl. Phys. **76**, 1503 (1994).
[80] T. Hanada, A. Yamana, Y. Nakamura, O. Nittono, and T. Wada, *Technical Digest: 9th International Photovoltaic Science and Engineering Conference* (International PVSEC-9, Tokyo, 1996), p. 595.
[81] W. Honel, G. Kuhn, and U.-C. Boehnke, Cryst. Res. Technol. **23**, 1347 (1988).
[82] L. S. Palatnik and E. I. Rogacheva, Neorg. Mater. **2**, 478 (1966).
[83] D. M. Ganbarov, G. G. Guseinov, and Z. Sh. Karaev, Neorg. Mater. **8**, 2211 (1972).
[84] C. Djega-Mariadassou, R. Lesueur, J. Leloup, and J. H. Albany, Phys. Lett. **65A**, 455 (1978).
[85] V. I. Tagirov, N. F. Gakhramanov, A. G. Guseinov, F. M. Aliev, and G. G. Guseinov, Sov. Phys. Crystallogr. **25**, 237 (1980).
[86] C. Djega-Mariadassou, A. Rimsky, R. Lesueur, and J. H. Albany, Jpn. J. Appl. Phys. **19**, 89 (1980).
[87] U.-C. Boehnke and G. Kuhn, J. Mater. Sci. **22**, 1635 (1987).
[88] H. W. Schock and L. Stolt, in *Proceedings of the 13th NREL Photovoltaics Program Review*, edited by H. S. Ullal and C. E. Witt (AIP, New York, 1995), p. 59.
[89] G. Dagan, F. Abou-Elfotouh, D. J. Dunlavy, R. J. Matson, and D. Cahen, Chem. Mater. **2**, 286 (1990).